Phase transition and thermodynamic properties of ThO_2: Quasi-harmonic approximation calculations and anharmonic effects*

Li Qiang(李 强)†, Yang Jun-Sheng(杨俊升), Huang Duo-Hui(黄多辉), Cao Qi-Long(曹启龙), and Wang Fan-Hou(王藩侯)

Computational Physics Key Laboratory of Sichuan Province, Yibin University, Yibin 644000, *China*

(Received 6 May 2013; revised manuscript received 5 July 2013; published 3 December 2013)

The thermodynamic properties and the phase transition of ThO_2 from the cubic structure to the orthorhombic structure are investigated using the first-principles projector-augmented wave method. The vibrational contribution to Helmholtz free energy is evaluated from the first-principles phonon calculations. The anharmonic contribution to quasi-harmonic free energy is accounted for by using an effective method (2010 *Phys. Rev. B* **81** 172301). The results reveal that at ambient temperature, the phase transition from the cubic phase to the orthorhombic phase occurs at 26.45 GPa, which is consistent with the experimental and theoretical data. With increasing temperature, the transition pressure decreases almost linearly. By comparing the experimental results with the calculation results, it is shown that the thermodynamic properties of ThO_2 at high temperature improve substantially after including the anharmonic correction to quasi-harmonic free energy.

Keywords: first-principles, ThO_2, phase transition, thermodynamic property, anharmonic correction

PACS: 71.15.Mb, 64.70.K–, 65.40.–b **DOI:** 10.1088/1674-1056/23/1/017101

1. Introduction

Thorium dioxide (ThO_2) has drawn considerable attention in recent years due to its usage as a nuclear material and solid-state electrolyte.[1,2] Moreover, owing to its prominent hardness, ThO_2 has potential applications as a high-k dielectric material and laser host.[3] At ambient pressure, ThO_2 is an important nuclear ceramic which exists in the fluorite structure with space group $Fm\bar{3}m$ (No. 225) up to its melting point at 3000 K. In spite of its interesting properties and high potential applications, the phase transition of ThO_2 is still inconclusive. A great deal of experimental and theoretical investigation has been devoted to solving this issue. Experimentally, high-pressure Raman spectra for ThO_2 were reported by Jayaraman *et al.*[4] They claimed the appearance of seven new Raman peaks near 30 GPa, testifying that ThO_2 starts to transform into an orthorhombic structure with space group *Pnma* (No. 62) at around 30 GPa. Idiri *et al.*[5] performed the compression experiments and observed that this phase transition really begins around 30 GPa, and that the two phases coexist in a wide pressure range of nearly 20 GPa. Dancausse *et al.*[6] investigated the pressure-induced phase transition from the cubic phase to the orthorhombic phase using the energy dispersive x-ray diffraction method. Their results suggested that ThO_2 undergoes a high-pressure-induced phase transformation from a cubic to an orthorhombic structural type at pressures of about 40 GPa; further, the high-pressure phase remains stable up to 55 GPa. Theoretically, Boettger *et al.*[7] performed the first-principles calculations using the relativistic linear combinations of a Gaussian type orbitals-fitting function technique and a predicted transition pressure of around 27.5 GPa. Moreover, based on first-principles density-functional theory, Wang *et al.*[8] predicted a single pressure induced structural transition of ThO_2 from the initial cubic structure to an orthorhombic structure around 26.5 GPa. Despite tremendous experimental and theoretical efforts, the pressure-induced phase transition remains one of the most controversial topics in the study of ThO_2.

At relatively low temperatures, the thermodynamic properties can be well predicted using the quasi-harmonic approximation (QHA)[9–13], in which only the volumetric effects on the phonon frequencies are taken into account. Obviously, QHA ignores the intrinsic anharmonic effects caused by phonon–phonon interaction. Since the anharmonicity becomes prominent at high temperature, QHA will not be good enough to predict the high-temperature thermodynamic properties. These effects have recently received a renewed interest.[14–16] An effective approach without requiring any adjustable parameter, proposed by Wu,[17] is adopted in this work to verify the occurrence of the pressure-induced phase transition from the cubic ThO_2 to the orthorhombic ThO_2 and evaluate the thermodynamic properties of both phases. The method can be thought of as an "improved" QHA. The applicability of this approach is demonstrated by applying it to MgO, ScN and YN.[14,15]

The rest of this paper is organized as follows. The theoretical methods are shown in Section 2. In Section 3, the calculation results are given and discussed. Finally, the con-

*Project supported by the National Natural Science Foundation of China (Grant No. 61275203), the Foundation of Sichuan Educational Committee, China (Grant Nos. 13ZA0198 and 13ZB0211), and the Foundation of Science and Technology of Yibin, China (Grant No. 2012SF034).

†Corresponding author. E-mail: wslypq@126.com

© 2014 Chinese Physical Society and IOP Publishing Ltd

clusions are drawn in Section 4.

2. Theoretical methods

The first-principles calculations are performed within the generalized gradient approximation (GGA) of a Perdew–Burke–Ernzerhof (PBE) functional,[18] as implemented in the Vienna *ab initio* simulation package (VASP).[19] The electron-ion interactions are treated within the projector-augmented wave.[20] For the Brillouin zone sampling, 9 × 9 × 9 and 9 × 15 × 4 Monkhorst–Pack meshes[21] are used for the cubic and orthorhombic ThO_2, respectively. The kinetic energy cutoff is 282.8 eV. The allowed error in the total energy is smaller than 10^{-3} eV per atom between two electronic self-consistent steps. The relaxation between two ionic steps will stop if all forces are smaller than -10^{-3} eV per atom. Thermodynamic calculations are performed by Phonopy.[22]

Within the framework of the quasi-harmonic approximation, the non-equilibrium Gibbs free energy $G(V,P,T)$ is usually given by[23]

$$G(V,P,T) = F_{\rm H}(V,T) + PV = E(V) + F_{\rm vib}(V,T) + PV, \quad (1)$$

where $F_{\rm H}(V,T)$ is the quasi-harmonic Helmholtz free energy; $E(V)$ represents the static energy from the first-principles total energy calculations fitted by an equation of state at 0 K and volume V; PV corresponds to the constant hydrostatic pressure condition; P is the pressure; and V is the volume.

The fully anharmonic Helmholtz free energy can be separated as[14]

$$H_{\rm A}(V,T) = F_{\rm H}(V,T) + F_{\rm anh}(V,T), \quad (2)$$

where $F_{\rm anh}(V,T)$ is the anharmonic correction to the quasi-harmonic Helmholtz free energy. QHA ignores the intrinsic phonon–phonon interaction, namely, the anharmonicity, which will lead to the case where the predicted properties, such as the thermal expansion coefficients, are much larger or smaller than the experimental data at high temperatures.[14] The temperature dependence of the phonon frequency is expressed in an implicit way in Wu and Wentzcovitch's method[14,17]

$$\Omega(V,T) = \omega(V'), \quad (3)$$

where ω is the phonon frequency from the first-principles calculations and Ω is the temperature-dependent phonon frequency used in quasi-harmonic formula of the free energy: Ω is not the renormalized phonon frequency. The relation of Ω with the renormalized phonon frequency was discussed in Ref. [14]. The temperature dependence of Ω is described by the temperature dependence of V' at a fixed volume V

$$V' = V\left|1 - C\frac{(V-V_0)}{V_0}\right|, \quad (4)$$

where C is a constant; V and V_0 are the predicted quasi-harmonic volumes at high and zero temperature under the same quasi-harmonic pressure; and V–V_0 is the volume expansion caused by the temperature. The method can be thought of as an "improved" QHA and works well while there is only one constant C,[14] $F_{\rm anh}(V,T)$ can be expressed in the following way:[17]

$$F_{\rm anh}(V,T) = \left[F_{\rm H}(V',T) - U_0(V')\right] - \left[F_{\rm H}(V,T) - U_0(V)\right], \quad (5)$$

where U_0 is the internal static energy, $F_{\rm anh}(V,T)$ can also be calculated through the first-principles molecular-dynamics (FPMD) simulation by

$$\begin{aligned} F_{\rm anh}(V,T) &= F_{\rm MD}(V,T) - F_{\rm H}(V,T) \\ &= \left[E_{\rm MD}(V,T) - TS_{\rm H}(V,T)\right] \\ &\quad - \left[E_{\rm H}(V,T) - TS_{\rm MD}(V,T)\right] \\ &\approx \left[E_{\rm MD}(V,T) - E_{\rm H}(V,T)\right], \end{aligned} \quad (6)$$

where $F_{\rm MD}$ is the free energy in FPMD; $E_{\rm MD}$ and $E_{\rm H}$ are the internal energy in FPMD and QHA, respectively; $S_{\rm MD}$ and $S_{\rm H}$ are the entropy in FPMD and QHA, respectively, which would be nearly equal at low temperature; and $F_{\rm anh}(V,T)$ can be calculated from one canonical ensemble FPMD simulation and further used to determine C through Eq. (5). FPMD is performed in the super cell with 96 atoms for cubic and orthorhombic ThO_2 with the same pseudopotential, exchange-correlation functional and cutoff energy. The Nosé mass controls the frequency of the temperature oscillations during the simulation.[19] For each simulation, 1-ps simulation is found to be long enough to calculate the ensemble average.

Based on the phonon density of states (DOS) $g(\omega)$, the vibrational free energy from the first-principles can be written as follows:[10]

$$F_{\rm vib}(V,T) = k_{\rm B}T\int_0^\infty \ln\left[2\sinh\frac{\hbar\omega}{2k_{\rm B}T}\right]g(\omega)\,{\rm d}(\omega), \quad (7)$$

where $k_{\rm B}$ is the Boltzmann constant; and ω and $\hbar$ are the phonon frequency and the reduced Planck constant, respectively. The non-equilibrium Gibbs function $G^*(V;P,T)$ can be minimized with respect to volume V

$$\left(\frac{\partial G^*(V;P,T)}{\partial V}\right)_{P,T} = 0. \quad (8)$$

The calculated static energies by first-principles with respect to the volume are fitted to the third-order Birch–Murnaghan equation of state[24]

$$\begin{aligned} E(V) &= E_0 + \frac{9V_0B_0}{16}\left\{\left[(V_0/V)^{2/3} - 1\right]^3 B_0' \right. \\ &\quad \left. + \left[(V_0/V)^{2/3} - 1\right]^2\left[6 - 4(V_0/V)^{2/3}\right]\right\}. \end{aligned} \quad (9)$$

Through "improved" QHA and QHA, the thermodynamic parameters of ThO_2 at any pressures and temperatures from the calculated energy-volume data at zero temperature and zero pressure can be obtained.

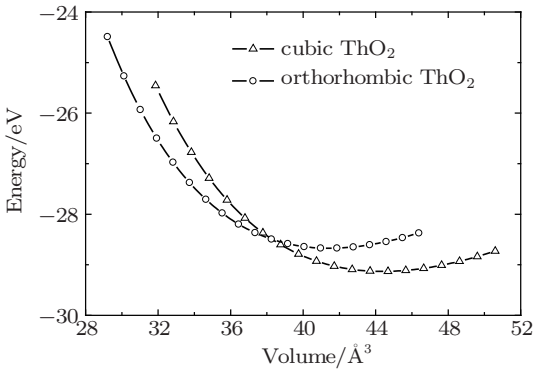


Fig. 1. Fitted total energy per formula unit as a function of volume for ThO_2 from third-order Birch–Murnaghan equation of state.

3. Results and discussion

3.1. Structural properties

Firstly, the appropriate cell parameters of ThO_2 have been obtained after optimizing the lattice constants and internal atom coordinates under the principle of energy minimization. Secondly, for cubic and orthorhombic ThO_2, a series of lattice constants are set to obtain the total energy E and the corresponding primitive cell volume V, then the E–V data are fitted to the third-order Birch–Murnaghan equation of state.[24] The results are shown in Fig. 1. From Fig. 1, the cubic ThO_2 is more stable than the orthorhombic ThO_2 at zero temperature and zero pressure, which accords with the experimental and theoretical data.[4,7] The calculated lattice parameter a_0, bulk modulus B_0 and its first derivate B_0' for both phases by the third-order Birch–Murnaghan equation of state are listed in Table 1, together with the available experimental and other theoretical data. It is obvious that our calculated results are in agreement with the other theoretical results[7,25–27] and experimental data.[2,5,28]

Table 1. Lattice constants, bulk modulus and its pressure derivation of the cubic and orthorhombic ThO_2.

	Cubic ThO_2				Orthorhombic ThO_2		
	This work	Other	Exp		This work	Other	Exp
		5.610[a]	5.600[d]	a/Å	6.103	6.122[f]	5.898[g]
a/Å	5.592	5.623[b]	5.598[e]	b/Å	3.716	3.749[f]	3.600[g]
		5.626[c]		c/Å	7.067	7.107[f]	6.862[g]
		198.2[f]	198[d]			163.2[f]	
B_0	187.6	184.5[c]	195[e]	B_0	202.1	206.8[c]	
		4.91[f]	4.6[d]			6.19[f]	
B_0'	4.19	4.49[c]	5.4[e]	B_0'	4.22	4.94[c]	

[a] Ref. [25], [b] Ref. [26], [c] Ref. [7], [d] Ref. [5], [e] Ref. [2], [f] Ref. [27], [g] Ref. [28].

3.2. Electronic structure

In the following, the electronic structures of cubic and orthorhombic ThO_2 at 0 GPa and 30 GPa are calculated and shown in Figs. 2(a) and 2(b), respectively. The Fermi level is set to zero. From Fig. 2(a), it can be seen that the low band in the range from −18.8 eV to −11.2 eV consists of O 2s and Th 6p states, which shows a clear hybridization. The high valence band in the range from −4.3 eV to 0 eV is mainly occupied by O 2p states with a little Th 6d and 5f states. Above the Fermi level, the conduction band is dominated by Th 5f states, mixed with a little Th 6d and O 2p states. The cubic ThO_2 shows a band gap of about 4.2 eV, which indicates that the cubic ThO_2 is a semiconductor. The electronic structure of orthorhombic ThO_2 is similar to the cubic ThO_2 except that it has a small band gap of 3.8 eV and the conduction band width becomes narrow due to the effect of pressure.

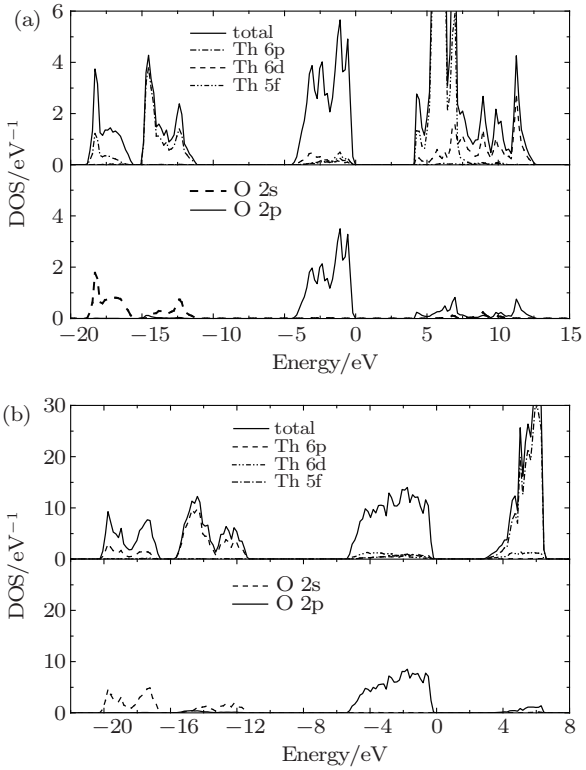


Fig. 2. Calculated total and partial density of states for cubic (a) and orthorhombic (b) ThO_2.

The values of C (see Eq. (4)) determined by FPMD are 0.17 and 0.21 for cubic and orthorhombic ThO_2, respectively, which are then used to construct the Gibbs free energy. Based on the perturbation theory, the lowest order term of the anharmonic contribution to free energy is proportional to T^2 at high temperatures.[14] Namely, $F_{\text{anh}} = bT^2$. The third and fourth order terms are usually small and can be ignored at high temperatures. Based on Eqs. (3)–(6), the anharmonic free energy correction of the cubic and orthorhombic ThO_2 at 0 GPa is displayed in Fig. 3. As shown in Fig. 3, the anharmonic free energy contribution in ThO_2 exhibits the typical T^2 behavior

at the applied temperatures. This is also true for Mg_2SiO_4 and MgO.[14,17] Moreover, it can be noted that the anharmonic contribution in cubic ThO_2 is smaller than that in orthorhombic ThO_2. This is due to the fact that the low-symmetry orthorhombic ThO_2 is the high pressure phase and has high anharmonicity at zero GPa.

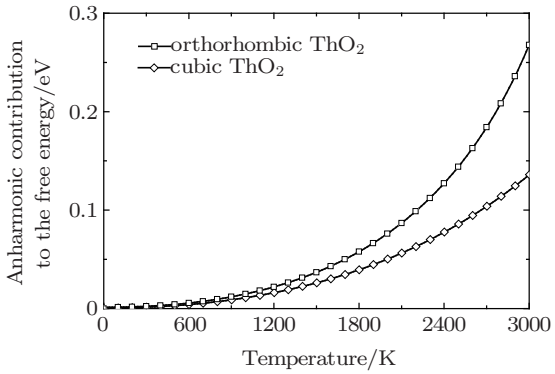


Fig. 3. Temperature dependence of the anharmonic contribution to the free energy at 0 GPa.

3.3. Phase transition

To clarify the phase transition of ThO_2 at any pressure and any temperature, more investigations are preformed using the "improved" QHA and QHA. It is well known that at the transition point, the Gibbs free energy of two phases are equal. Therefore, the phase transition pressure and temperature from the cubic ThO_2 to the orthorhombic ThO_2 can be evaluated from the usual condition of equal Gibbs energies, i.e., the pressure, at which the Gibbs energies are the same for both phases.

The differences in Gibbs free energy between the cubic and orthorhombic ThO_2, $\Delta G = G_{Pnma} - G_{Fm-3m}$, predicted by the "improved" QHA and QHA, are shown in Figs. 4(a) and 4(b) for different temperatures and pressures, respectively. From Figs. 4(a) and 4(b), it is found that when $P = 27.06$ GPa, $\Delta G = 0$. This means that at zero temperature, the transition pressure from the cubic ThO_2 to the orthorhombic ThO_2 is 27.06 GPa, which is consistent with the theoretical results;[7] also, the cubic ThO_2 is more stable than the orthorhombic ThO_2 when the pressure is below 27.06 GPa. At zero temperature, the transition pressure calculated by the "improved" QHA and QHA is the same, which is due to the disappearance of the anharmonic effect at the applied temperature. At 300 K, the transition pressure obtained from the "improved" QHA is 26.45 GPa, which is close to the QHA value of 26.70 GPa and the experimental value.[4] When the temperature increases to 1500 K, the value of the transition pressure of 22.78 GPa, predicted by the "improved" QHA, is somewhat smaller than the value of 23.61 GPa predicted by QHA. When the temperature is fixed, ΔG increases with the pressure decreasing, which means that the cubic ThO_2 becomes more and more stable compared with the orthorhombic ThO_2. At zero pressure, ΔG is positive in the range of 0 K–3000 K, which implies that the cubic phase is more stable than the orthorhombic phase and the phase transition would not occur even at 3000 K when the pressure is below 18.66 GPa obtained by "improved" QHA and 19.70 GPa obtained by QHA. Moreover, it can be observed that the transition pressure decreases almost linearly with the temperature increasing above room temperature. Thus, though the anharmonic contribution to free energy plays an important role in the phase transition of ThO_2, the phase transition pressure predicted by the "improved" QHA and QHA are almost the same at the applied temperature and the discrepancies between both approaches are less than 1.2 GPa.

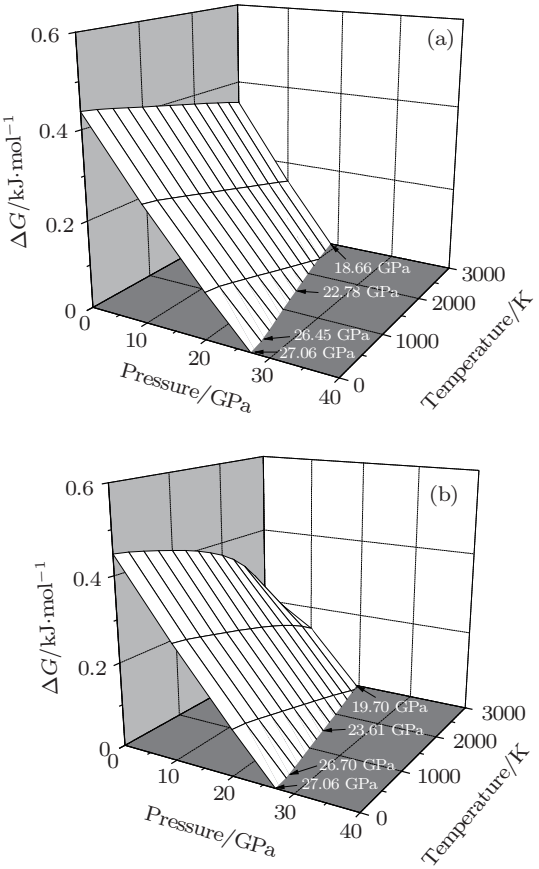


Fig. 4. The dependence of ΔG on temperature and pressure for (a) "improved" QHA and (b) QHA.

3.4. Thermodynamic properties

Within the framework of the density functional perturbation theory (DFPT), phonon dispersion curves of both phases are calculated and shown in Figs. 5(a) and 5(b). As seen in Fig. 5, the absence of any imaginary phonon frequency in the whole Brillouin zone for cubic and orthorhombic ThO_2 gives direct proof of their dynamical stabilities at the given condition. The predicted phonon dispersion curves of cubic ThO_2 accord with the experimental data[29] at low frequency, but slight deviations can be observed at high frequency, which are mainly due to the current calculation based on the harmony

approximation at 0 K, while the experimental measurements are performed at room temperature and the anharmonic effect could be induced by a higher temperature. Moreover, it can be noted that the highest phonon frequency of the orthorhombic phase is larger than that of the cubic phase, which is due to the shorter bond lengths of the orthorhombic phase that contribute to higher phonon frequencies.

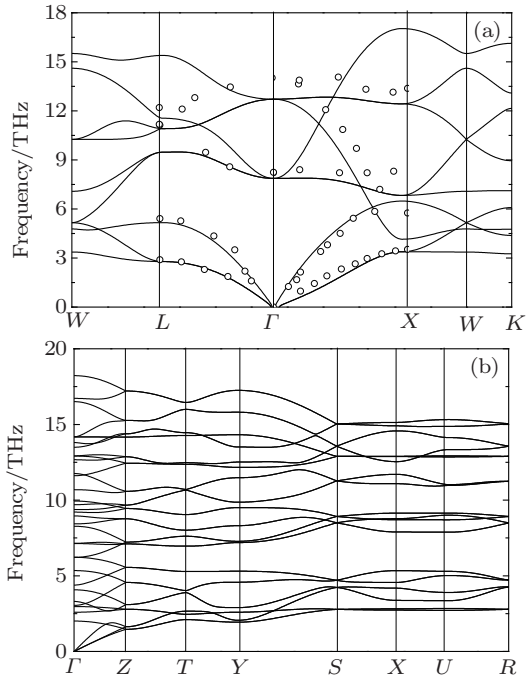


Fig. 5. Calculated phonon dispersion curves for (a) cubic and (b) orthorhombic ThO_2 at the theoretical equilibrium volumes, together with the room measurements (symbols) of cubic ThO_2.

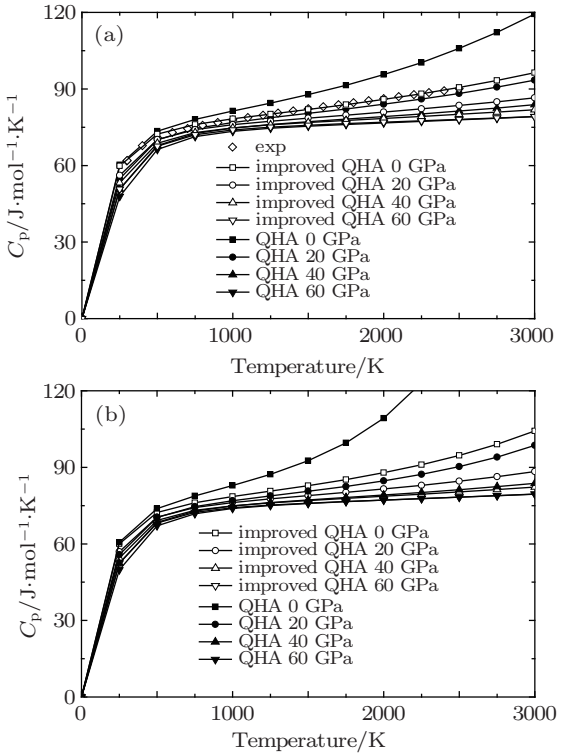


Fig. 6. Calculated heat capacity of (a) cubic and (b) orthorhombic ThO_2 at different pressures, together with the experimental data.

Thermodynamic properties play an important role in understanding the thermal response of materials. The heat capacities of the cubic and orthorhombic ThO_2 at constant pressure, predicted by the "improved" QHA and QHA, are shown in Figs. 6(a) and 6(b), respectively, compared with the experimental data.[30] From Fig. 6, it can be seen that the heat capacity C_P of both phases at different pressures increases steeply below 300 K, then the increasing trend becomes gentler at high temperatures. At zero GPa, the "improved" QHA predicted C_p for cubic ThO_2 in a range from 600 K to 2500 K is closer to the experimental data than that obtained from QHA. Thus, after including the anharmonic correction to quasi-harmonic free energy, the heat capacity of ThO_2 is depicted well by the "improved" QHA.

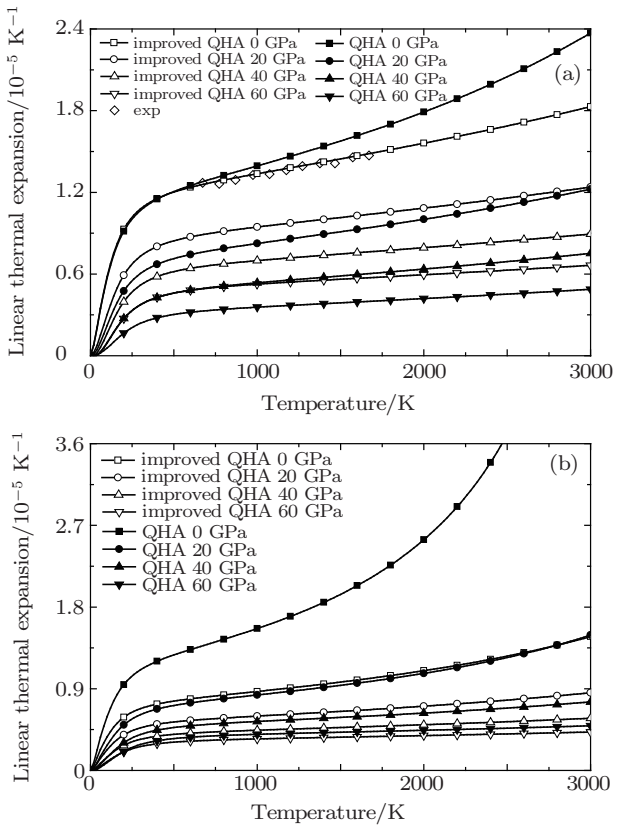


Fig. 7. Calculated linear thermal expansion coefficients of (a) cubic and (b) orthorhombic ThO_2 in comparison with experimental data.

ThO_2 is a potential optical component material and laser host and hence, it is necessary to investigate its thermal expansion coefficient. The calculated pressure and temperature dependences of the linear thermal expansion coefficient α of the cubic and orthorhombic ThO_2 are plotted in Figs. 7(a) and 7(b), respectively. From Fig. 7, it can be seen that as the temperature increases, the linear thermal expansion coefficient of both phases increases rapidly below 300 K and then gradually turns into a slower increase at high temperatures. At the same pressure, the cubic phase has a slightly lower thermal expansion coefficient than the orthorhombic phase. At zero pressure, the linear thermal expansion coefficient α of cubic

ThO_2 calculated by the "improved" QHA is consistent with the experimental data;[31] QHA significantly underestimates the thermal expansion coefficient of both phases. Therefore, after inclusion of anharmonic effects, the "improved" QHA improves significantly the thermodynamic properties of ThO_2 at high temperatures.

4. Conclusions

The thermodynamic properties and the phase transition from the cubic ThO_2 to the orthorhombic ThO_2 are studied using the first-principles projector-augmented wave method. According to the usual condition of equal Gibbs energy, the phase transition from the cubic ThO_2 to the orthorhombic ThO_2 occurs at 26.45 GPa, which is in agreement with the experimental and theoretical data. The transition pressure decreases almost linearly with the applied temperatures above room temperature. At zero pressure, the predicted heat capacity and linear thermal expansion coefficient of cubic ThO_2 are consistent with the experimental data. By comparing the experimental results with the calculation results, it is shown that the thermodynamic properties of ThO_2 improve considerably after inclusion of the anharmonic effects.

References

[1] Xiao H Y, Zhang Y and Weber W J 2012 *Phys. Rev. B* **86** 054109
[2] Staun O J, Gerward L, Kanchana V and Vaitheeswaran G 2004 *J. Alloy. Compd.* **381** 37
[3] Linares R C 1967 *J. Phys. Chem. Solids* **28** 1285
[4] Jayaraman A, Kourouklis G A and van Uitert L G1988 *Pramana* **30** 225
[5] Idiri M, Le Bihan T, Heathman S and Rebizant J 2004 *Phys. Rev. B* **70** 014113
[6] Dancausse J P, Gering E, Heathman S and Benedict U 1990 *High Pressure Res.* **2** 381
[7] Boettger J C 2009 *Int. J. Quantum Chem.* **109** 3564
[8] Wang B T, Shi H, Li W D and Zhang P 2010 *J. Nucl. Mater.* **399** 181
[9] Li Q, Huang D H, Cao Q L and Wang F H 2013 *Chin. Phys. B* **22** 037101
[10] Li Q, Huang D H, Cao Q L, Wang F H, Cai L C, Zhang X L and Jing F Q 2012 *Chin. Phys. B.* **21** 127102
[11] Luo F, Cai L C, Chen X R, Jing F Q and Alfe D 2012 *J. Appl. Phys.* **111** 053503
[12] Ren D H and Cheng X L 2012 *Chin. Phys. B* **21** 127103
[13] Yu Y, Zhao B, Zhu S, Gao T, Hou H and He Z 2013 *Physica B* **417** 83
[14] Wu Z and Wentzcovitch R M 2009 *Phys. Rev. B* **79** 104304
[15] Tahri S, Qteish A, Al-Qasir I I and Meskini N 2012 *J. Phys.: Condens. Matter* **24** 035401
[16] Grabowski B, Ismer L, Hickel T and Neugebauer J 2009 *Phys. Rev. B* **79** 134106
[17] Wu Z 2010 *Phys. Rev. B* **81** 172301
[18] Perdew J P, Burke K and Ernzerhof M 1996 *Phys. Rev. Lett.* **77** 3865
[19] Kresse G and Joubert D 1999 *Phys. Rev. B* **59** 1758
[20] Blöchl P E 1994 *Phys. Rev. B* **50** 17953
[21] Monkhorst H J and Pack J D 1976 *Phys. Rev. B* **13** 5188
[22] Togo A, Oba F and Tanaka I 2008 *Phys. Rev. B* **78** 134106
[23] Otero-de-la-Roza A, Abbasi-Pérez D and Luaña V 2011 *Comput. Phys. Commun.* **182** 2232
[24] Birch F 1947 *Phys. Rev.* **71** 809
[25] Kanchana V, Vaitheeswaran G, Svane A and Delin A 2006 *J. Phys.: Condens. Matter* **18** 9615
[26] Shein I, Shein K and Ivanovskii A 2007 *J. Nucl. Mater.* **361** 69
[27] Boudjemline A, Louail L, Islam M M and Diawara B 2011 *Comput. Mater. Sci.* **50** 2280
[28] Duclos S J, Vohra Y K, Ruoff A L, Jayaraman A and Espinosa G P 1988 *Phys. Rev. B* **38** 7755
[29] Clausen K, HayesW, Macdonald J E, Osborn R, Schnabel P G, HutchingsMT and Magerl A 1987 *Journal of the Chemical Society, Faraday Transactions 2: Molecular and Chemical Physics* **83** 1109
[30] Barin I 1995 *Thermochemical Data of Pure Substances* (3rd edn.) (Germany: Verlagsgesellschaft bmH Weinheim) p. 1657
[31] Mann M, Thompson D, Serivalsatit K, Tritt T M, Ballato J and Kolis J 2010 *Cryst. Growth Des.* **10** 2146